OPEN

Assessment of Virtual Monoenergetic Images in Run-off Computed Tomography Angiography: A Comparison Study to Conventional Images From Spectral Detector Computed Tomography

Haiyan Ren, MM, Yanhua Zhen, MM, Zheng Gong, MD, Chuanzhuo Wang, MD, Zhihui Chang, MD, and Jiahe Zheng, MD

Objective: The aims of this study were to evaluate image quality of virtual monoenergetic images (VMIs) compared with conventional images (CIs) from spectral detector CT (SDCT) and to explore the optimal energy level in run-off computed tomography angiography (CTA).

Methods: The data sets of 35 patients who received run-off CTA on the SDCT were collected in this retrospective study. Conventional images were generated via iterative reconstruction algorithm and VMI series from 40 to 120 keV were generated via spectral reconstruction algorithm. The objective indices including vascular attenuation, noise, signal-to-noise ratio, and contrast-to-noise ratio were compared. Two readers performed subjective evaluation using a 5-point scale.

Results: The attenuation showed higher values compared with CIs at 40 to 60 keV ($P < 0.001$). The noise was similar in 60- to 80-keV VMIs and significantly decreased in 90- to 120-keV VMIs ($P < 0.001$) in comparison with CIs. The signal-to-noise ratio and contrast-to-noise ratio were improved in 40- to 60-keV VMIs compared with CIs ($P < 0.05$). The score of subjective assessment was higher than that of CIs in 50- to 70-keV VMIs ($P < 0.001$).

Conclusions: Virtual monoenergetic images can provide improved image quality compared with CIs from SDCT in run-off CTA, and VMIs at 60 keV may be the best choice in evaluating lower extremity arteries.

Key Words: spectral detector CT, virtual monoenergetic images, angiography

(*J Comput Assist Tomogr* 2021;45: 232–237)

The run-off computed tomography angiography (CTA) has been widely applied for convenient, noninvasive reliability in detecting arterial stenoses and becomes an alternative diagnostic method compared with digital subtraction angiography.[1–4] With the development of technology, spectral CT, such as dual-source and rapid kV switching scanner, has been widely used, which can generate virtual monoenergetic images (VMIs) with spectral discrimination achieved at the source level as well as improve vessels contrast and provide extra information for diagnosis.[5] Currently, the spectral detector computed tomography (SDCT) is applied in clinical practice. The CT scanner innovatively realizes energy separation based on detectors, which can simultaneously obtain dual-energy projection data at the same spatial and temporal resolution, and then VMIs can be obtained by linear combination of these dual-energy data sets, which resembles true monoenergetic images and shows more advantages in decreasing artifact and noise.[6–14]

Several studies have reported the advantages of VMIs on the SDCT for optimizing the image quality of coronary artery.[15,16] So far, the only 1 study in run-off CTA on the SDCT was about evaluating the stent visualization, which showed that VMIs could obtain more accurate stent lumen evaluation compared with 120-kVp polychromatic conventional images (CIs).[11] However, the potential benefits of VMIs for evaluating lower extremity vessels have not yet been reported. Therefore, we hypothesized that VMIs could provide improved image quality in comparison with CIs for assessing lower extremity arteries on the SDCT.

The current study aimed at comparing the image quality of VMIs and CIs from the SDCT and exploring the optimal energy level of VMIs in run-off CTA.

MATERIALS AND METHODS

This retrospective study got the approval of institutional review board, and informed consent was waived. The data sets of 35 patients who received run-off CTA on the SDCT (IQon; Philips Healthcare, the Netherlands) in our hospital because of suspected lower extremity arteriosclerosis obliterans were collected from January 2019 to October 2019, including 24 male and 11 female patients, with a mean age of 67.3 ± 8.4 years, ranging 47.0 to 86.0 years.

Computed Tomography Scanning Protocol

All examinations were performed in a craniocaudal direction and covered the distal abdominal aorta to the toes on the SDCT. Ninety milliliter of iodinated contrast agent (iohexol, 350 mgI/mL, Beilu Pharmaceutical Co, Ltd, Beijing, China) was injected intravenously for all patients at a flow rate of 4 mL/s, followed by injecting saline of 30 mL. Scans were triggered with the bolus-tracking technique and were initiated 16 seconds after the attenuation of the distal abdominal aorta reached 150 HU. The following image acquisition parameters were used: slice collimation, 64 × 0.625 mm; rotation time, 0.5 seconds; pitch, 0.96; matrix, 512 × 512; dose modulation type, DoseRight 3D-DOM (Philips Healthcare); and tube voltage, 120 kVp.

From the Department of Radiology, Shengjing Hospital of China Medical University, Shenyang, China.

Received for publication June 17, 2020; accepted October 8, 2020.

Correspondence to: Jiahe Zheng, MD, 36, Sanhao St, Heping District, Shenyang City, China (e-mail: zhengjh120624@126.com).

This study was supported by the Science and Technology Project of Liaoning Province, China (the Liaoning Natural Science Foundation Guidance Plan, Grant 2019-ZD-0776).

The authors declare no conflict of interest.

DOI: 10.1097/RCT.0000000000001126

TABLE 1. Objective Analysis Results

		CI	40 keV	50 keV	60 keV	70 keV	80 keV	90 keV	100 keV	110 keV	120 keV
CIA	CT, HU	422.9 ± 71.9	1320.3 ± 237.8↑	861.9 ± 151.9↑	592.4 ± 101.5↑	430.6 ± 71.3	329.3 ± 52.6↓	263.1 ± 40.5↓	218.2 ± 32.4↓	186.5 ± 26.9↓	163.6 ± 23.0↓
	Noise, HU	15.0 ± 2.6	18.8 ± 6.2↑	15.5 ± 4.0	13.8 ± 3.0	12.8 ± 2.5	12.4 ± 2.4	12.1 ± 2.3↓	11.9 ± 2.3↓	11.9 ± 2.3↓	11.7 ± 2.2↓
	SNR	29.8 ± 7.4	76.6 ± 19.3↑	59.3 ± 19.3↑	45.4 ± 11.2↑	35.2 ± 8.8	28.0 ± 7.2	22.9 ± 5.9↓	19.3 ± 4.9↓	16.6 ± 4.2↓	14.7 ± 3.7↓
	CNR	25.8 ± 6.9	71.8 ± 18.5↑	54.5 ± 13.9↑	40.6 ± 10.7↑	30.5 ± 8.2	23.4 ± 6.5	18.3 ± 5.2↓	14.7 ± 4.2↓	12.1 ± 3.5↓	10.2 ± 3.0↓
CFA	CT, HU	427.1 ± 78.8	1280.6 ± 236.9↑	837.4 ± 152.7↑	576.9 ± 103.2↑	420.5 ± 73.5	324.0 ± 54.2↓	258.5 ± 43.1↓	215.0 ± 35.1↓	185.9 ± 32.2↓	162.3 ± 25.5↓
	Noise, HU	12.7 ± 2.4	20.5 ± 8.7↑	15.6 ± 5.2↑	12.9 ± 3.3	11.5 ± 2.3	10.7 ± 2.0	10.2 ± 1.9↓	9.9 ± 1.9↓	9.74 ± 1.9↓	9.6 ± 1.9↓
	SNR	36.0 ± 10.7	72.4 ± 21.2↑	59.3 ± 15.6↑	47.8 ± 12.0↑	38.9 ± 10.1	32.2 ± 8.5	27.2 ± 7.5↓	23.3 ± 6.5↓	20.7 ± 6.1↓	18.4 ± 5.4↓
	CNR	31.2 ± 9.9	68.2 ± 20.4↑	54.7 ± 14.8↑	42.8 ± 11.3↑	33.7 ± 9.3	26.8 ± 7.7	21.6 ± 6.6↓	17.6 ± 5.6↓	14.9 ± 5.2↓	12.6 ± 4.0↓
MSFA	CT, HU	425.3 ± 94.3	1217.5 ± 266.3↑	797.3 ± 171.6↑	550.3 ± 116.0↑	401.9 ± 82.6	312.2 ± 61.6↓	248.3 ± 48.5↓	207.1 ± 39.4↓	178.1 ± 33.1↓	157.0 ± 28.7↓
	Noise, HU	16.3 ± 9.4	41.3 ± 31.5↑	27.8 ± 19.9↑	20.0 ± 13.1	15.5 ± 9.1	12.8 ± 6.7	11.1 ± 5.3	10.0 ± 4.4	10.1 ± 5.2	8.7 ± 3.7
	SNR	33.2 ± 14.8	42.0 ± 19.5	39.6 ± 18.2	36.7 ± 16.9	33.6 ± 15.7	31.6 ± 17.2	27.9 ± 12.7	25.6 ± 11.7	22.3 ± 9.9	22.4 ± 10.2
	CNR	29.5 ± 13.3	39.7 ± 18.4↑	36.7 ± 16.9	33.1 ± 15.4	29.4 ± 13.9	26.8 ± 15.2	22.8 ± 10.6	20.0 ± 9.4↓	16.7 ± 7.7↓	16.1 ± 7.5
MPA	CT, HU	397.2 ± 104.6	1106.4 ± 301.6↑	724.6 ± 195.3↑	500.4 ± 132.5↑	365.9 ± 95.0	281.9 ± 72.7↓	226.9 ± 56.5↓	189.5 ± 46.2↓	163.2 ± 39.1↓	144.1 ± 33.9↓
	Noise, HU	19.4 ± 11.9	55.9 ± 36.7↑	36.4 ± 23.5↑	25.1 ± 15.7	18.3 ± 11.0	14.1 ± 8.1	11.5 ± 6.2	9.7 ± 5.0↓	8.5 ± 4.1↓	7.7 ± 3.6↓
	SNR	28.8 ± 21.1	31.9 ± 30.7	30.7 ± 27.3	29.3 ± 24.1	27.8 ± 20.1	26.4 ± 16.6	25.1 ± 13.1	24.1 ± 11.2	23.4 ± 9.7	22.6 ± 8.7
	CNR	24.6 ± 18.4	30.0 ± 29.0	28.1 ± 25.3	26.0 ± 21.7	23.6 ± 17.5	21.5 ± 13.9	19.3 ± 10.5	17.6 ± 8.4	16.1 ± 7.0	14.7 ± 5.8
TPT	CT, HU	383.2 ± 79.7	1025.8 ± 218.7↑	679.7 ± 141.1↑	476.1 ± 96.1↑	353.9 ± 69.9	277.4 ± 54.3↓	227.5 ± 44.9↓	193.4 ± 39.2↓	169.6 ± 35.5↓	152.1 ± 32.9↓
	Noise, HU	24.9 ± 12.9	70.2 ± 37.1↑	46.3 ± 23.8↑	32.0 ± 16.0	23.4 ± 11.4	18.2 ± 8.6	14.8 ± 6.9	12.5 ± 5.7↓	10.9 ± 5.0↓	9.7 ± 4.7↓
	SNR	19.7 ± 11.5	20.4 ± 15.5	20.0 ± 14.1	19.5 ± 12.4	19.0 ± 10.5	18.5 ± 8.7	18.3 ± 7.7	18.1 ± 6.7	18.1 ± 6.1	18.0 ± 5.7
	CNR	17.1 ± 10.0	19.0 ± 14.5	18.2 ± 12.9	17.2 ± 10.9	16.2 ± 8.9	15.1 ± 7.1	14.2 ± 5.9	13.4 ± 5.0	12.8 ± 4.2	12.1 ± 3.7
Mean	CT, HU	412.9 ± 73.3	1196.9 ± 214.6↑	784.5 ± 138.3↑	542.1 ± 93.4↑	396.6 ± 66.5	306.6 ± 49.2↓	246.1 ± 39.1↓	205.6 ± 31.8↓	177.4 ± 27.3↓	156.5 ± 23.1↓
	Noise, HU	17.6 ± 5.6	41.0 ± 19.0↑	28.1 ± 11.9↑	20.6 ± 7.8	16.2 ± 5.3	13.6 ± 3.8	11.9 ± 2.9↓	10.8 ± 2.3↓	10.2 ± 2.1↓	9.5 ± 1.8↓
	SNR	29.7 ± 6.6	49.4 ± 14.0↑	42.3 ± 11.0↑	36.1 ± 8.8↑	31.1 ± 7.1	27.5 ± 6.2	24.4 ± 4.7↓	22.1 ± 4.1↓	20.2 ± 3.7↓	19.2 ± 3.5↓
	CNR	25.7 ± 6.0	46.4 ± 13.4↑	38.9 ± 10.3↑	32.2 ± 8.1↑	26.9 ± 6.3	22.8 ± 5.5	19.3 ± 4.0↓	16.7 ± 3.3↓	14.5 ± 2.9↓	13.1 ± 2.6↓

Values are expressed as mean ± SD.

↑and ↓ indicate that the values of VMIs were significantly increased and decreased compared with CI, respectively.

CFA indicates common femoral arteries; CIA, common iliac artery; MPA, middle popliteal arteries; MSFA, middle superficial femoral arteries; TPT, tibioperoneal trunk.

Image Reconstruction

The slice thickness and increment were both 1 mm for image reconstruction. Conventional images were generated via iterative reconstruction algorithm (iDose4, level 3) and VMIs series ranging from 40 to 120 keV (10-keV intervals) were reconstructed via spectral reconstruction algorithm (Spectral B, level 3). Images over 120-keV energy levels were not evaluated because vascular enhancement becomes fainter with higher-energy levels.[17] Then, all images were sent to the workstation (IntelliSpace Portal 9.0, Philips Healthcare). Maximum intensity projections and curved planar reformation were reconstructed for per patient. Window settings (width, 350; level, 45) were preseted but freely modifiable.

Objective Analysis

Measurements were completed by a reader with 3 years of experience in CTA. The mean vascular attenuation was obtained after measuring on the transverse images 3 times in bilateral common iliac arteries, common femoral arteries, middle superficial femoral arteries, middle popliteal arteries, and tibioperoneal trunk. The standard deviation (SD) of vascular attenuation was recorded as image noise, and the attenuation of adjacent muscle at the same transverse section was recorded for the calculation of the signal-to-noise ratio (SNR) and contrast-to-noise ratio (CNR), which were obtained by the formulas: $SNR = HU_{vessel}/noise_{vessel}$, $CNR = (HU_{vessel} - HU_{muscle})/noise_{vessel}$.[18,19] Target areas were set at the center of the vessels and were maximized within the luminal diameter, avoiding vascular walls, atherosclerotic plaques, and calcifications. Besides, severe stenosis or occlusive target arteries were excluded.

Subjective Analysis

The subjective evaluation was completed individually by 2 readers with 8 and 11 years of experience in CTA. The CIs and VMIs series, including transverse, maximum intensity projection, and curved planar reformation images, were scored using a 5-point scale by following parameters: noise, artifacts, contrast, and sharpness, and were scored from 1 = poor to 5 = perfect. The detailed scoring criteria were as described in our previous study.[18] The final score was decided by consensus under the circumstance of disagreement between the 2 readers.

Statistical Analysis

All data set analysis was completed by SPSS (Version 23.0) and GraphPad Prism (Version 8.0). Quantitative variables were expressed as mean ± SD and compared by analysis of variance. Furthermore, objective indices of CIs and VMIs series were compared with Dunnett multiple comparison post hoc test. Qualitative variables were expressed as median with interquartile and compared with the Kruskal-Wallis test. Significance was defined as a P value of less than 0.05. Cohen κ test was used to assess the interobserver agreement, as proposed in the prior study.[18,20]

RESULTS

Objective Analysis

Table 1 shows the results of objective image quality indices. The vascular attenuation, noise, SNR, and CNR showed a similar trend which decreased with energy levels increasing (Figs. 1, 2). The mean vascular attenuation showed significantly higher values in 40- to 60-keV VMIs than those of CIs ($P < 0.001$) and increased approximately 190.3%, 90.0%, and 31.3% at 40, 50, and 60 keV, respectively. The mean vascular attenuation was similar to CIs in 70-keV VMIs ($P > 0.05$). At 80 to 120 keV, the mean attenuation was lower compared with CIs ($P < 0.001$). The mean noise showed significantly higher values in 40- to 50-keV VMIs ($P < 0.05$) and similar to CIs in 60- to 80-keV VMIs ($P > 0.05$) and significantly lower than that of CIs at 90 to 120 keV ($P < 0.001$). The mean SNR and CNR were both significantly higher in 40- to 60-keV VMIs ($P < 0.05$), which increased

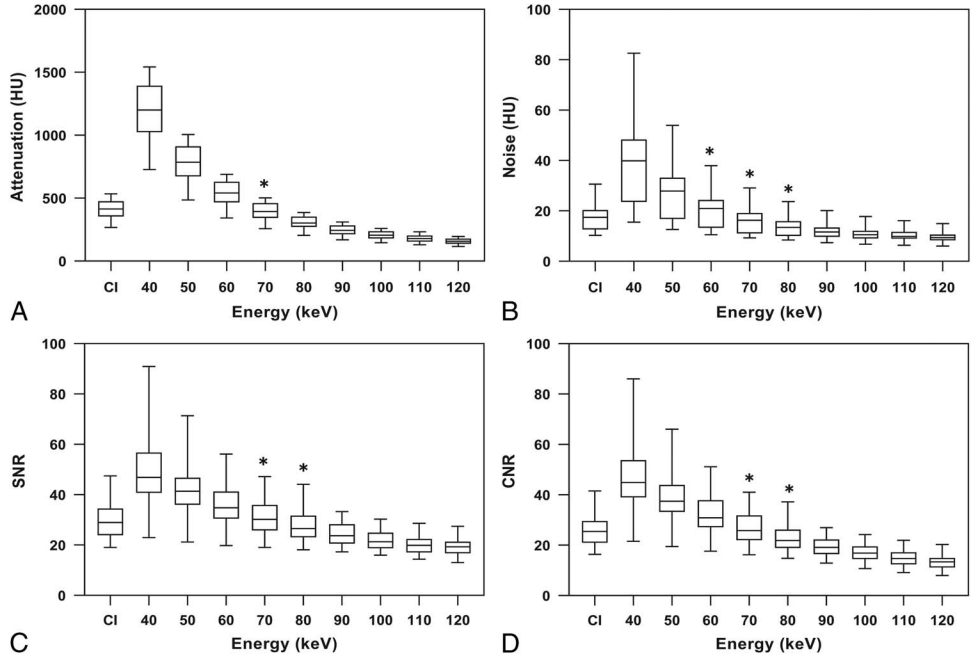

FIGURE 1. Box-and-whisker plots comparing results of the mean vascular attenuation (A), noise (B), SNR (C), and CNR (D) in VMIs from 40 to 120 keV and CIs. The results showed a similar trend, which decreased with the energy levels increasing. The difference was significant except * between VMIs and CIs.

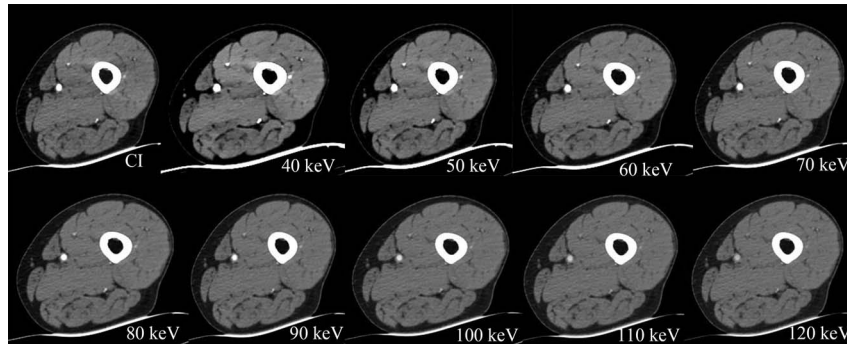

FIGURE 2. Axial images at middle superficial femoral arteries of CIs and VMIs ranging from 40 to 120 keV. The vascular attenuation and noise were decreased with energy levels increasing in VMIs.

approximately 66.3%, 42.4%, and 21.5% at 40, 50, and 60 keV in terms of SNR, respectively, and 80.5%, 51.4%, and 25.3% at 40, 50, and 60 keV in terms of CNR, respectively. At 70 to 80 keV, the mean SNR and CNR were similar to CIs and showed lower values compared with CIs at 90 to 120 keV ($P < 0.05$).

Subjective Analysis

Results of the subjective analysis are presented in Table 2, and representative images are shown in Figure 3. The score was lower than that of CIs in 40-keV VMIs ($P = 0.007$) and showed higher values in 50- to 70-keV VMIs ($P < 0.001$) and were equivalent to CIs in 80-keV VMIs ($P = 0.317$) and 90-keV VMIs ($P = 0.025$) and lower than that of CIs in 100 to 120 keV ($P < 0.001$). The interobserver agreement between the 2 readers was good to excellent (range, κ values > 0.61).

DISCUSSION

This study showed that the mean vascular attenuation, SNR, CNR, and subjective image quality were improved at 50 to 60 keV, and the noise was similar to CIs in 60-keV VMI, whereas the noise significantly increased at 50 keV. Although all objective indices were higher compared with CIs in 40-keV VMI, the subjective evaluation was inferior to CIs. Besides, objective indices in 70-keV VMIs were similar to CI, whereas subjective evaluation was superior to CIs. Objective indices and subjective image quality scores were similar or decreased compared with CIs in 80- to 120-keV VMIs.

The previous studies showed that low energy levels VMIs (≤60 keV) on the SDCT could obviously improve abdominal vascular contrast for higher photoelectric attenuation as the energies close to the K-edge of iodine.[8,21] The present study demonstrated a similar result that the attenuation of lower extremity vessels was higher at 40 to 60 keV compared with CIs. The ability to improve vascular contrast in low energy levels VMIs is useful in the circumstance of suboptimal vascular enhancement, which can avoid extra contrast medium and radiation doses brought by extra scanning and especially benefit patients with renal dysfunction.

In the present study, among all energy levels VMI, the attenuation, SNR, and CNR showed the highest values at 40 keV, whereas the score of subjective image quality was inferior to CI, which may be resulted from the obviously increased noise at lower energy levels.[22] The scores of subjective assessment showed the highest values in 50- and 60-keV VMIs with significantly improved SNR and CNR, whereas the noise was higher at 50 keV and equal at 60 keV compared with CIs. A recent study[11] also reported that the highest attenuation, SNR, and CNR of the in-stent lumen and adjacent vessel in lower extremity were shown, whereas the stent visualization was inferior to CIs in 40-keV VMIs on the SDCT. In addition, the study demonstrated that the attenuation, SNR, and CNR were significantly improved at 50 to 70 keV. However, the highest score in subjective analysis showed at 90 keV with significantly decreased SNR and CNR compared with CIs, which was different from our result. The possible reason was that the image quality of vessels with a stent was influenced not only by SNR and CNR but also by the stent beaming hardening.[11] Thus, the optimal image quality should depend on the balance of attenuation, contrast, and noise, etc.[22]

Sudarski et al[22] reported that the SNR and CNR showed significantly higher values in 60-keV VMIs in comparison with CIs in run-off CTA on a dual-source CT, whereas these were comparable in 40- to 50-keV VMIs. In the present study, the SNR and CNR showed significantly higher values at 40 to 60 keV and the subjective image quality score was significantly higher than that of CIs in 50 to 70 keV. The difference of results may be due to the different physics way for acquiring the image data and the different reconstruction methods for generating VMIs in per scanner.[23]

There are several limitations as follows. First, only evaluations of image quality were performed. The diagnostic accuracy of images in comparison with digital subtraction angiography should be taken into consideration in further study. Second, the sample size may not large enough and larger samples are required to warrant our results. Third, the energy interval is 10 keV in this study and further work should use a smaller interval.

TABLE 2. Subjective Analysis Results

	Image Quality	*P*	κ
CI	4 (4–4)		0.656
40 keV	3 (3–4)	0.007	0.824
50 keV	5 (5–5)	<0.001	0.646
60 keV	5 (5–5)	<0.001	n/a
70 keV	4 (4–5)	<0.001	0.775
80 keV	4 (4–4)	0.317	0.623
90 keV	4 (4–4)	0.025	0.777
100 keV	4 (3–4)	<0.001	0.913
110 keV	3 (3–3)	<0.001	n/a
120 keV	3 (2–3)	<0.001	0.721

Values are expressed as median with interquartile; *P* values were the results of comparison among VMIs from 40 to 120 keV and CIs.

n/a indicates not applicable.

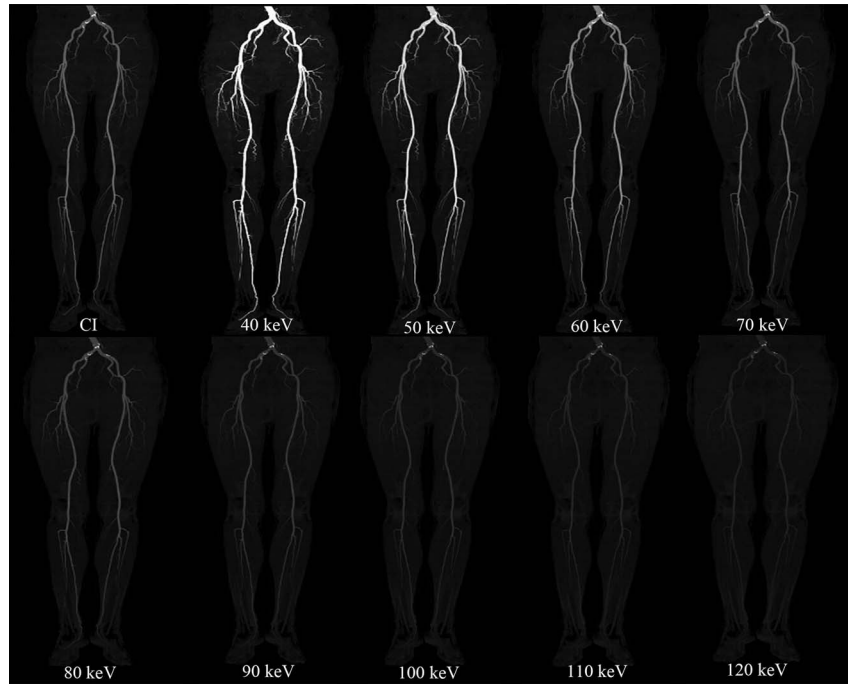

FIGURE 3. Maximum intensity projection images of CIs and VMIs ranging from 40 to 120 keV were shown as examples. Virtual monoenergetic images at 50 and 60 keV showed the highest subjective image scores, which were both 5.

In conclusion, the present study shows that VMIs derived from SDCT can provide improved vascular contrast, SNR, CNR, as well as better subjective image quality in comparison with CIs in run-off CTA. The VMIs at 60 keV has the highest subjective image quality score with significantly improved attenuation, SNR, CNR, and similar noise, which shows the potential advantages in improving visualization and diagnostic confidence of vascular stenosis.

REFERENCES

1. Schernthaner R, Stadler A, Lomoschitz F, et al. Multidetector CT angiography in the assessment of peripheral arterial occlusive disease: accuracy in detecting the severity, number, and length of stenoses. *Eur Radiol*. 2008;18:665–671.
2. Mangold S, De Cecco CN, Schoepf UJ, et al. A noise-optimized virtual monochromatic reconstruction algorithm improves stent visualization and diagnostic accuracy for detection of in-stent re-stenosis in lower extremity run-off CT angiography. *Eur Radiol*. 2016;26:4380–4389.
3. Qi L, Zhao Y, Zhou CS, et al. Image quality and radiation dose of lower extremity CT angiography at 70 kVp on an integrated circuit detector dual-source computed tomography. *Acta Radiol*. 2015;56:659–665.
4. Duan Y, Wang X, Yang X, et al. Diagnostic efficiency of low-dose CT angiography compared with conventional angiography in peripheral arterial occlusions. *AJR Am J Roentgenol*. 2013;201:W906–W914.
5. Ananthakrishnan L, Rajiah P, Ahn R, et al. Spectral detector CT-derived virtual non-contrast images: comparison of attenuation values with unenhanced CT. *Abdom Radiol (NY)*. 2017;42:702–709.
6. Hickethier T, Baeßler B, Kroeger JR, et al. Monoenergetic reconstructions for imaging of coronary artery stents using spectral detector CT: in-vitro experience and comparison to conventional images. *J Cardiovasc Comput Tomogr*. 2017;11:33–39.
7. Goo HW, Goo JM. Dual-energy CT: new horizon in medical imaging. *Korean J Radiol*. 2017;18:555–569.
8. Doerner J, Wybranski C, Byrtus J, et al. Intra-individual comparison between abdominal virtual mono-energetic spectral and conventional images using a novel spectral detector CT. *PLoS One*. 2017;12:e0183759.
9. Kalisz K, Rassouli N, Dhanantwari A, et al. Noise characteristics of virtual monoenergetic images from a novel detector-based spectral CT scanner. *Eur J Radiol*. 2018;98:118–125.
10. Neuhaus V, Abdullayev N, Große Hokamp N, et al. Improvement of image quality in unenhanced dual-layer CT of the head using virtual monoenergetic images compared with polyenergetic single-energy CT. *Invest Radiol*. 2017;52:470–476.
11. Zhang D, Xie Y, Wang Y, et al. Initial clinical experience of virtual monoenergetic imaging improves stent visualization in lower extremity run-off CT angiography by dual-layer spectral detector CT. *Acad Radiol*. 2020;27:825–832.
12. Große Hokamp N, Gilkeson R, Jordan MK, et al. Virtual monoenergetic images from spectral detector CT as a surrogate for conventional CT images: unaltered attenuation characteristics with reduced image noise. *Eur J Radiol*. 2019;117:49–55.
13. Reimer RP, Flatten D, Lichtenstein T, et al. Virtual monoenergetic images from spectral detector CT enable radiation dose reduction in unenhanced cranial CT. *AJNR Am J Neuroradiol*. 2019;40:1617–1623.
14. Sellerer T, Noël PB, Patino M, et al. Dual-energy CT: a phantom comparison of different platforms for abdominal imaging. *Eur Radiol*. 2018;28:2745–2755.
15. Van Hedent S, Große Hokamp N, Kessner R, et al. Effect of virtual monoenergetic images from spectral detector computed tomography on coronary calcium blooming. *J Comput Assist Tomogr*. 2018;42:912–918.
16. Yi Y, Zhao XM, Wu RZ, et al. Low dose and low contrast medium coronary CT angiography using dual-layer spectral detector CT. *Int Heart J*. 2019; 60:608–617.

17. Wichmann JL, Gillott MR, De Cecco CN, et al. Dual-energy computed tomography angiography of the lower extremity runoff: impact of noise-optimized virtual monochromatic imaging on image quality and diagnostic accuracy. *Invest Radiol*. 2016;51:139–146.

18. Liu B, Gao S, Chang Z, et al. Lower extremity CT angiography at 80 kVp using iterative model reconstruction. *Diagn Interv Imaging*. 2018; 99:561–568.

19. Almutairi A, Sun Z, Poovathumkadavi A, et al. Dual energy CT angiography of peripheral arterial disease: feasibility of using lower contrast medium volume. *PLoS One*. 2015;10:e0139275.

20. Kundel HL, Polansky M. Measurement of observer agreement. *Radiology*. 2003;228:303–308.

21. Yuan R, Shuman WP, Earls JP, et al. Reduced iodine load at CT pulmonary angiography with dual-energy monochromatic imaging: comparison with standard CT pulmonary angiography—a prospective randomized trial. *Radiology*. 2012;262:290–297.

22. Sudarski S, Apfaltrer P, Nance JW Jr., et al. Optimization of keV-settings in abdominal and lower extremity dual-source dual-energy CT angiography determined with virtual monoenergetic imaging. *Eur J Radiol*. 2013; 82:e574–e581.

23. van Hamersvelt RW, Eijsvoogel NG, Mihl C, et al. Contrast agent concentration optimization in CTA using low tube voltage and dual-energy CT in multiple vendors: a phantom study. *Int J Cardiovasc Imaging*. 2018; 34:1265–1275.